

# Contact Wrench Space Stability Estimation for Humanoid Robots

Robert W. Ellenberg  
Drexel University  
rwe24@drexel.edu

Paul Y. Oh  
Drexel University  
pyo22@drexel.edu

**Abstract**—To execute ladder climbing motions effectively, a humanoid robot requires a reliable estimate of stability. Traditional methods such as Zero Moment Point are not applicable to vertical climbing, and do not account for force limits imposed on end effectors. This paper implements a simple contact wrench space method using a linear combination of contact wrenches. Experiments in simulation showed ZMP equivalence on flat ground. Furthermore, the estimator was able to predict stability with four point contact on a vertical ladder. Finally, an extension of the presented method is proposed based on these findings to address the limitations of the linear combination.

## I. INTRODUCTION

Search and rescue is an application for humanoid robotics that has received significant attention in both popular media and literature. Industrial disasters such as the Fukushima Daichi reactor explosion can trap people, and require expert help to resolve. Rather than put humans in danger, a humanoid rescue robot can withstand radiation, chemical, and biological agents. A humanoid robot's build is a natural fit for human environments as well.

In particular, ladders are a common feature in factories and navy ships. A small mobile robot would have great difficulty navigating a steep ladder. A humanoid has a natural advantage due to the size and form factor. As humanoid robots such as ATLAS, S-one, and DRC-Hubo are developed towards search as rescue work, ladders will become an important challenge to overcome.

Ladder climbing in many ways represents the next big problem to solve in humanoid robotics. Unlike walking and stair-climbing, the majority of movement in ladder climbing is lifting or lowering the robot's weight. The robot is supported with both feet and hands, and in the case of ladders with safety cages (Figure 1), cannot depend on climbing with feet alone.

To plan and execute climbing motions effectively, this problem requires a means of estimating stability that accounts for support from the robot's hands and feet simultaneously. In [1], a statically stable planner was demonstrated that used statically stable trajectories. Since it is possible to alternate between three and four-point contact, static stability can be maintained if contacts are stable. To satisfy the assumptions of the planner, however, the robot must be able to maintain contact with the ladder when needed. Failure to measure and react to loss of contact can mean losing support and falling from the ladder.

---

This work was supported in part by the Defense Advanced Research Projects Agency (DARPA) award #N65236-12-1-1005 for the DARPA Robotics Challenge.



Fig. 1. An example of a ladder with safety cage for equipment access.

This paper introduces an implementation for a humanoid robot stability estimator using Contact Wrench Space methods. Section II surveys similar methods of stability estimation and the limitations of these methods when applied to ladder climbing. Section III explains the contact wrench sum formulation as applied to a humanoid robot with articulated fingers. Section IV shows simulation results showing correspondence with the ZMP metric during flat-ground contact. Section V shows simulation results of measurement of four-point contact stability on a vertical ladder. Finally, Section VI summarizes findings and future directions.

## II. HUMANOID STATE ESTIMATION

State estimation has been a part of robotics for many years. Biped robot state estimation started with the use of Linear Inverted Pendulum Models (LIPM) and (Zero Moment Point) ZMP control, in works such as [2], in which IMU and force-torque sensors are used to estimate the ZMP of a biped robot. They used a Kalman filter to refine the pose estimate, which is a common feature in these works. For example, [3] introduces a 2D biped model that uses a lumped mass model to predict model states for the sagittal plane.

The goal for a state estimator usable for climbing trajectories is to measure the space of possible contact forces that the robot can exert at any time. While instantaneous force/torque

information from a wrist or foot may reveal the current state of reaction forces, they do not directly measure what reaction forces are possible under changing conditions.

The Linear Inverted Pendulum Model (LIPM) and Zero Moment Point (ZMP) concepts introduced in [4] solved this problem for the case of uniform terrain. ZMP-based methods have since been demonstrated with humanoids such as ASIMO, Hubo, HRP, and Wabian. A ZMP measurement from a robot's force-torque sensors predicts how close to instability a robot is as a function of both its current pose, but also the robot's dynamics. The limitation of ZMP-based methods, however, is that the simplified model assume a constant center of mass height. While this is adequate for piecewise-flat terrain like stairs, ladder-climbing operates largely in the vertical direction.

A more advanced method of stability checking draws inspiration from support grasps, or grasps which use passive forces to achieve force closure [5]. The forces and torques applied to an object being grasped are known as contact wrenches, and the combined effect of all of these is known as the Contact Wrench Space. Originally introduced in [6] for rough-terrain walking, this method consists of building a six-dimensional space of wrenches applied to the robot due to each contact. For a given robot pose, if a linear combination of these wrenches can be applied to oppose the robot's weight, then the current pose is stable.

In [7], this concept was applied to a humanoid robot to calculate a CWS for a humanoid robot based on foot contacts. This method applied a modified version of the GJK algorithm for the interior check. Critically, this method introduced the use of polyhedral cones to describe the contact wrench space. Treating contact normal force as infinite allowed a significant increase in calculation speed. When applied to "strong" limbs like a humanoid robot's legs, then this simplification is reasonable, since the strength limits of a leg are not often exceeded during statically stable motions.

For ladder-climbing, however, this assumption can mean overestimating the strength of dexterous hands, leading to grip failure. On the DRC Hubo humanoid for example, the rated grip strength is approximately  $15kgF$  perpendicular, approximately %30 of the robot's weight. On a vertical ladder, the moment created due to the robot's distance from the ladder must be matched by the grip strength of the hands. This grip force limit means that some grip locations lead to overly high grip forces, and some motions may put too much load on one gripper. Therefore, for ladder climbing, the stability estimate must account for force limits at each end effector.

### III. CONTACT WRENCH SUM FORMULATION

The contact wrench sum concept is based on grasp-planning work such as [8], in which optimal contact locations are calculated to provide force closure around an object. A contact wrench is a combination of the contact force  $f$  and the moment  $\tau$  with respect to a fixed point  $P_0$ . Together, the force and moment create a wrench that can be applied to the object. A contact wrench  $w_i$  is compactly expressed in the form of (1). The Contact Wrench Space is therefore a volume in the six-dimensional force / moment space that contains every possible

combination of these wrenches. Dimensions such as volume and minimum diameter of this wrench space have been used to obtain quality metrics of grasps in work such as [9] and [10].

$$\begin{pmatrix} \vec{f}_i \\ r_{i/0_{COM}} \times \vec{f} \end{pmatrix} \quad (1)$$

These methods can also be applied to the robot itself, which was the major contribution of [6] and [7]. Much as a grasped object is stabilized if an arbitrary disturbance can be opposed, a multi-limbed robot can be considered to be stable if a disturbance wrench  $\vec{w}_d$  lies within the contact wrench space. The disturbance wrench consists of several components:

- Inertial wrench  $\vec{w}_i$ : the equivalent wrench due to the robot's inertia and overall linear and angular acceleration.
- Gravity wrench  $\vec{w}_g$  due to the weights of each robot link.
- External applied load  $\vec{w}_f$  due to applied forces or carried load.

The disturbance wrench in (2) can be simplified to (3) if motion is quasi-static, and no external loads are applied to the robot. The moment of the gravity wrench  $\vec{w}_g$  is taken with respect to a fixed origin, which can without loss of generality be fixed to a point on the robot.

$$\vec{w}_d = \vec{w}_i + \vec{w}_g + \vec{w}_f \in \Sigma \vec{w}_i \quad (2)$$

$$\vec{w}_g = \begin{pmatrix} -m\vec{g} \\ \vec{r}_{G/0} \times -m\vec{g} \end{pmatrix} \quad (3)$$

To account for friction forces, the friction cone of each contact can be approximated as a 4-sided friction pyramid, as introduced in [6]. Assume a limiting normal force  $f_n^i$  for each point contact, a friction coefficient of  $\mu^i$  per contact  $i$ , the friction pyramid is represented by the four contact forces in (4). The basis vectors  $\hat{b}_j$  lie in the null plane of the contact normal, spaced  $\frac{\pi}{2}rad$  apart.

$$\vec{f}_i = \vec{f}_n + \hat{b}_j \mu_i f_n, j = 1..4 \quad (4)$$

Evaluating stability from the contact wrench space and a known disturbance wrench reduces to an interior point check. If  $-\vec{w}_d$  lies within the CWS volume, then the robot's reaction forces can oppose the disturbance. The general procedure is:

- 1) Build a list of contact points, normals, and friction coefficients.
- 2) For each contact, create a set of contact forces including normal force and friction force perpendicular to the normal.
- 3) Compute the contact wrench for each of these possible forces by (1).
- 4) Build a 6D convex hull of these contact wrenches.
- 5) Perform an interior point check on the CWS and  $\vec{w}_d$ .

Note that the contact wrench space in this method is a linear combination of contact wrenches. When sufficient strength can be assumed, then the magnitude of contact forces is normalized. While this approach is typical for grasping, it

presents certain challenges when applied to a humanoid robot. If the Contact Wrench Space is formulated without force limits, then a pose such as (Figure 2) will be considered stable, despite the high forces applied to the fingers to keep from falling backwards.

#### Hubo in simulation hanging from ladder with fingers

Fig. 2. Example of a pose that depends on limited grip strength for balance.

In (5), a simple planar model approximates grip force  $F_{grip}$ . For a grasp height  $h = 1m$ , a body overhang  $d = .3m$ , and a lumped mass  $m = 48kg$ , the grip force required is approximately  $14.3kgF$ , which is very close to maximum straight-pull rating of  $15kgF$ . This pose is typical of ladder climbing while facing forward due to knee clearance.

Therefore, the assumption of either a uniform contact force, or infinite maximum normal force as in [7] have the potential to produce false positive estimates of stability.

$$F_{grip} = \frac{mgd}{h} \quad (5)$$

A simple interior check algorithm used to prototype the algorithm was used in python. Given that each facet of the convex hull represents a hyperplane in 6D, any interior point in the convex hull will satisfy (6), where  $V$  is the point in question,  $x$  is the normal vector of the facet's hyperplane, and  $b$  is the offset from the origin for the hyperplane. This information is available as part of the qhull convex hull solution. Therefore, an easy way to check that a point is interior is to iterate over the list of facets. This procedure requires  $O(n)$  time for a success, and worst-case  $O(n)$  for a failure.

$$Vx + b \leq 0 \quad (6)$$

#### A. Simulation in OpenHubo

The simulation used for these experiments was the open source OpenHubo<sup>1</sup> platform. Based on the OpenRAVE environment, openHubo adds important simulation elements such as servo control, along with a complete dynamic model of Hubo2 and DRC Hubo robots. These robot models and the OpenHubo simulator have been employed in [11] and [12] for evaluation of locomotion planning, and in [13] to plan throwing trajectories.

The DRC Hubo humanoid (figure 3) was modeled in OpenHubo by deriving rigid body masses and inertias from a detailed CAD model in SolidWorks. The model was exported to Universal Robot Description Format (URDF) via the SolidWorks URDF exporter plugin. The URDF model was then converted to OpenRAVE XML format for use with OpenHubo via a python module included in OpenHubo. Model geometry was exported as shrinkwrapped STL models for each rigid link, which were then manually decomposed into convex sub-bodies using the STL-VRML toolbox for MATLAB<sup>2</sup>. Model specifications for the DRC Hubo are given in Table I.

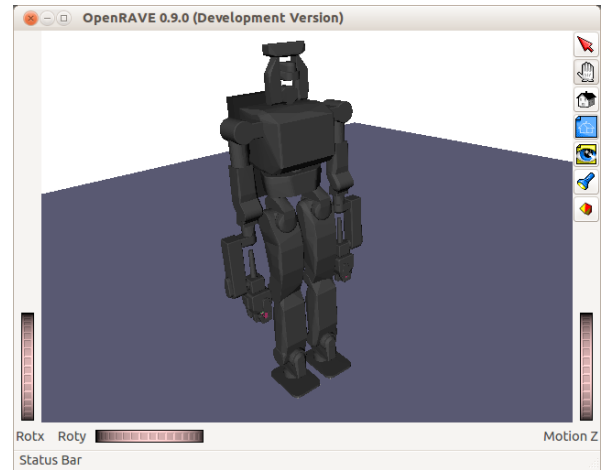


Fig. 3. DRC Hubo and OpenHubo model

TABLE I. LINK LENGTHS AND MASSES FOR DRC HUBO ROBOT

Link	Length	Mass
Torso	290mm	12kg
Upper Leg	350mm	5.1kg
Lower Leg	350mm	4.0kg
Foot (length)	220mm	2.2kg
Foot (width)	110mm	-
Upper Arm	250mm	3.5kg
Lower Arm	250mm	2kg

#### B. Contact Measurement

When estimating contact and contact forces in simulation, one challenge that arises with Open Dynamics Engine (ODE) is collision handling. Contact restoring force is proportional to penetration depth between two bodies. However, a large articulated system such as a humanoid creates closed kinematic chains, leading to constraint loops that cause solution instability. The result of this is that bodies in contact will not settle to an equilibrium position, but instead “jitter” in place slightly. In a given simulation step, only part of a body may be penetrating, even though on average full contact is made.

The physical DRC Hubo has rubber pads on the feet and fingers to add a small amount of compliance when grasping objects or placing a foot. Shifting the robot’s weight between front and rear extremes can cause compression of approximately  $1mm$ . While soft contact is not supported currently in OpenRAVE with ODE, the effect was approximated by the addition of rectangular primitive contact bodies on the hands and feet. These bodies are fixed to the robot’s hands and feet. During solution however, fixed constraints are relaxed slightly to allow quicker convergence. Typically these primitive bodies yield 4-8 collision points, instead of tens of points as would be measured with a detailed mesh model (Figure 4).

Directly querying contact locations abstracts away the role of F/T sensors in these experiments. However, a set of contact points is similar to the information that would be gathered from an array of simple two-state touch sensors on the hands and feet. Since a precise reaction force is not required, this simplification was considered to be a minor abstraction. A motion planner typically uses contact checking as an easy

<sup>1</sup><https://github.com/dasrobotics/openHubo>

<sup>2</sup><http://github.com/robEllenberg/stl-vrml-toolbox>



Fig. 4. Comparison of contacts detected with trimesh-primitive (upper) collision vs. primitive-primitive (lower) collision. Fewer discrete contacts reduce computational burden during convex hull generation.

failure metric, yet at the same time we need those contacts to determine probably reaction forces. A simple solution to this issue for planning is to treat the contact pads as solid objects only during execution. The assumption here is that the thickness of the contact pads represents the maximum reasonable deflection those pads are expected to undergo, and can therefore be ignored during motion planning.

For a single contact pad, this definition is somewhat loose, in that contact could be achieved on one edge of the pad, while the majority remains out of contact. This could be resolved by partitioning the contact body into discrete segments. Unfortunately, simply partitioning the contact body itself leads to increased noise and jitter due to the smaller mass and inertia of each individual piece. Due to the inherent tradeoffs in ODE, the stiffness of the contact relative to the mass/inertia of the body is a major factor in the uncertainty of the contacts. This does add an additional 6DOF to the total solution for ODE, however. This type of optimization of computational efficiency is outside the scope of this work.

#### IV. COMPARISON TO ZMP

An initial experiment demonstrates the close correspondence between the CWS prediction and the simulation results for the static case. For this experiment, the robot was biased to lean forward at the hips and ankles, with the torso remaining perpendicular to the ground. The arms were tilted at the shoulder at an angle  $\theta$ , which shifts the center of mass towards the front of the robot. Figure 5 shows the predicted vs. actual failure point for a nearly static case for varying torso offsets. The initial pose for the robot is given in Table IV. The angle at which the robot fell forward was determined via a bisection algorithm. The prediction from the CWS was recorded before running the dynamic simulation, and the resulting success for failure was logged for each joint angle. For this planar case,



Fig. 5. Balance failure point from simulation compared to prediction from CWS.

TABLE II. INITIAL POSE FOR FORWARD TILT EXPERIMENT

Joint	Angle (deg)
Hip Pitch	$-9.1^\circ$
Ankle Pitch	$9.1^\circ$
Shoulder Pitch Min	$-11.5^\circ$
Shoulder Pitch Max	$-32.1^\circ$

no false positive predictions of stability were observed. While the robot physically fell forward at an arm angle greater than  $.560rad$ , the CWS predicted failure for tilt angles greater than  $0.546rad$ , a margin of approximately 2.5%.

#### V. STABILITY DURING LADDER CLIMBING

Earlier work on ladder climbing in [1] assumed that the contact directions were fixed for a given grasp. For the case of hand grips on ladder rungs, this meant the contact forces were pointed outward towards the robot, while foot contacts were assumed to be vertical. While this adequately characterized the balance that should be achievable with the ideal pose, if the grasp or foot placement varied, then the contact conditions would not match the planned path. Due to the limiting grip strength, even small errors in grip placement could lead to loss of grip.

Maximum torque for each joint of DRC Hubo's fingers was calculated in (7). Maximum finger torque  $\tau_f$  is determined from the total pull force  $F_{pull}$ , the number of fingers per hand  $n_f$ , and the experimentally-determined effective finger length  $L_f$ . For a  $12kgF$  pull force, the minimum finger torque for a stable grip in simulation was determined to be  $1.5Nm$ .

$$\tau_f = L_f F_{pull} / n_f \quad (7)$$

TABLE III. TABLE OF LIMITS FOR LADDER POSE TRIALS

Parameter	Min	Max
Torso distance from ladder	0.25m	0.65m
Grasp point above rung	0.09m	0.11m
Foot placement spacing	0.24m	-
Palm yaw angle from +Y	60°	-

TABLE IV. SCALING OF FORCE LIMITS FOR 4-POINT CONTACT

Foot Force Scale	Finger Force Scale	Prediction
-	1.0	False
-	2.0	False
-	3.0	False
-	4.0	False
-	5.0	False
8.0	6.0	False
6.0	7.0	True
4.0	8.0	True
3.0	9.0	True

One challenge of predicting contact forces is that the robot is over-constrained. Because DRC Hubo is position-controlled with high gains, small errors in hand or foot placement can lead to large internal forces and uneven contacts.

A ladder grasping pose with four points of contact was planned using a whole-body inverse kinematics solver. The numerical inverse-jacobian inverse kinematics solver in the CoMPS library [14]. Grasp and foot placement positions were first approximated with manual goal transforms that place the end effectors within 5mm of the goal point. A bisection algorithm was then used to close each grasp and foot contact to within a joint angle tolerance of 0.001rad.

Table III explains the bounds on body posture relative to the ladder that were used for this experiment. Table IV shows the required scale factors on finger force and foot force to correctly predict a supporting condition. The contact wrenches were each iteratively scaled up until a solution was found, or a scale factor of 10 was reached. Finger torque was adjusted to less than 10% excess for the pose, ensuring that the robot could barely maintain stability in the four-point contact pose.

These results are consistent with what would be expected from a linear combination of contacts. Support must come from a combination of each end-effectors, yet the contact wrench space only encloses a linear combination of contact forces. To be physically consistent, the coefficients must all be less than unity. However, this restriction means that the net force predicted from both hands will never exceed a single finger's maximum force, and typically be much less. In fact, stability is only correctly predicted when each finger can exert a total force equivalent to both hands combined (scale factor of 6). Maximum force from each foot must be similarly scaled up. This result is a fundamental limitation on the predictive power of a linear combination of contact forces.

The solution Unfortunately, the number of points in the Minkowski sum grows very rapidly as the number of contacts  $n$  increases, and as the number of cone facets  $r$  increases. The total number of vertices in the Minkowski sum that forms the CWS is given by (8). This equation predicts, for example, that a complete CWS for 4 contact points with 4 facets each will have a total of 191 points. By contrast, if friction is assumed to be small ( $\mu_i = 0$ ), then only 15 points are required to define

the CWS, which takes less than 1ms using the same setup.

$$V = \sum_{k=1}^n \binom{k+r-1}{k} \binom{n}{k} \quad (8)$$

Table V itemizes the total points required to form the full Minkowski sum for the DRC Hubo model. Constructing the complete Minkowski sum from each individual link is prohibitively complex. However, by taking a convex hull of contact wrenches at each end-effector, the total number of points in the sum is reduced by a factor of 4000 in the worst case.

TABLE V. MINKOWSKI SUMS OVER RIGID LINK CONVEX HULLS VS END-EFFECTOR CONVEX HULLS

Body	Minimum Contacts	Friction	CWS points	Sum over links	Sum over end-effectors
leftFoot	4	y	16	16	16
rightFoot	4	y	16	288	288
leftPalm	2	y	8	2600	2600
rightPalm	2	y	8	23408	23408
Body_LF12	1	n	1	46817	-
Body_LF13	1	n	1	93635	-
Body_LF22	1	n	1	187271	-
Body_LF23	1	n	1	374543	-
Body_LF32	1	n	1	749087	-
Body_LF33	1	n	1	1498175	-
Body_RF12	1	n	1	2996351	-
Body_RF13	1	n	1	5992703	-
Body_RF22	1	n	1	11985407	-
Body_RF23	1	n	1	23970815	-
Body_RF32	1	n	1	47941631	-
Body_RF33	1	n	1	95883263	-

This process can be further simplified by creating a minimal-friction representation of contact forces. Because the friction component of the contact force is perpendicular to the normal vector, it does not contribute to the moment of the contact wrench. If contacts are culled via convex hull on contact forces, rather than contact wrenches, then a minimum of four contact wrenches are required for a given end effector with friction. This simplification would reduce the number of points needed to 9800 for the DRCHubo.

## VI. CONCLUSIONS AND FUTURE WORK

This paper has verified that a contact wrench sum is equivalent to ZMP in the case of flat level ground. Furthermore, this method allows estimation of stability in multi-limb contact without a-priori knowledge of contact directions. Finally, experiments with four-point contact have shown that a linear combination of contact wrenches can predict stability. However, the maximum contact forces require unreasonable scaling to do so. This points to a fundamental limitation of linear combinations when maximum contact force is not uniform.

Further development of this work will explore partial Minkowski sums of contact wrenches. Particularly for weaker contacts such as gripper surfaces, the Minkowski sum will account for total forces from multiple simultaneous contacts. Simultaneously, this method should limit single contact forces to a physically realistic value. Predictions for ideal grip vs.

reduced grip strength due to contact failure will be compared to tabulate prediction accuracy vs. computational cost. Coupled with a fast interior-check algorithm, this method could be fast enough to be generated online.

## REFERENCES

- [1] Y. Zhang, J. Luo, K. Hauser, R. Ellenberg, P. Oh, A. Park, M. Paldhe, and C. G. Lee, "Geometric constraints for ladder climbing for humanoid robots," in *Proceedings of TePRA*, 2013.
- [2] I. Hashlamon and K. Erbatur, "Center of mass states and disturbance estimation for a walking biped," in *Mechatronics (ICM), 2013 IEEE International Conference on*, 2013, pp. 248–253.
- [3] W. Wang and Y. Li, "Path planning for redundant manipulator without explicit inverse kinematics solution," in *Robotics and Biomimetics (ROBIO), 2009 IEEE International Conference on*, 2009, pp. 1918–1923.
- [4] M. Vukobratovic, A. Frank, and D. Juricic, "On the stability of biped locomotion," *Biomedical Engineering, IEEE Transactions on*, vol. BME-17, no. 1, pp. 25–36, 1970.
- [5] M. Wang and Y.-H. Liu, "Force passivity in fixturing and grasping," in *Robotics and Automation, 2003. Proceedings. ICRA '03. IEEE International Conference on*, vol. 2, 2003, pp. 2236–2241 vol.2.
- [6] H. Hirukawa, S. Hattori, K. Harada, S. Kajita, K. Kaneko, F. Kanehiro, K. Fujiwara, and M. Morisawa, "A universal stability criterion of the foot contact of legged robots - adios zmp," in *Robotics and Automation, 2006. ICRA 2006. Proceedings 2006 IEEE International Conference on*, may 2006, pp. 1976 –1983.
- [7] Y. Zheng, M. Lin, D. Manocha, A. Adiwahono, and C.-M. Chew, "A walking pattern generator for biped robots on uneven terrains," in *Intelligent Robots and Systems (IROS), 2010 IEEE/RSJ International Conference on*, oct. 2010, pp. 4483 –4488.
- [8] C. Borst, M. Fischer, and G. Hirzinger, "Grasp planning: how to choose a suitable task wrench space," in *Robotics and Automation, 2004. Proceedings. ICRA '04. 2004 IEEE International Conference on*, vol. 1, april-1 may 2004, pp. 319 – 325 Vol.1.
- [9] J. Weisz and P. Allen, "Pose error robust grasping from contact wrench space metrics," in *Robotics and Automation (ICRA), 2012 IEEE International Conference on*, 2012, pp. 557–562.
- [10] Y. Zheng, M. C. Lin, and D. Manocha, "On computing reliable optimal grasping forces," *Robotics, IEEE Transactions on*, vol. 28, no. 3, pp. 619 –633, june 2012.
- [11] K. Sohn and P. Oh, "Applying human motion capture to design energy-efficient trajectories for miniature humanoids," in *Intelligent Robots and Systems (IROS), 2012 IEEE/RSJ International Conference on*, 2012, pp. 3425–3431.
- [12] Y. Jun and P. Oh, "A 3-tier infrastructure: Virtual-, mini-, online-hubo stair climbing as a case study," in *International Association of Science and Technology for Development-Robo2011*, Pittsburgh, PA, November 2011.
- [13] D. Lofaro and P. Oh, "Humanoid throws inaugural pitch at major league baseball game: Challenges, approach, implementation and lessons learned," in *Intelligent Robots and Systems (IROS), 2012 IEEE/RSJ International Conference on*, nov. 2012.
- [14] D. Berenson, S. Srinivasa, and J. Kuffner, "Task space regions: A framework for pose-constrained manipulation planning," *International Journal of Robotics Research (IJRR)*, vol. 30, no. 12, pp. 1435–1460, October 2011.